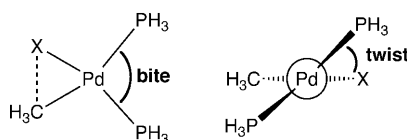


## The Steric Nature of the Bite Angle

Willem-Jan van Zeist, Ruud Visser, and F. Matthias Bickelhaupt\*<sup>[a]</sup>

Catalytic activity is known to depend on the ligand–metal–ligand angle, the so-called bite angle (see Scheme 1).<sup>[1]</sup> Many pioneering studies have been undertaken



Scheme 1. Bite angle (left) and twist angle (Newman projection, right) in the TS of an oxidative insertion [Eq. (1)].

in order to understand how exactly reaction barriers are affected by this and related structural parameters of the catalytically active complex.<sup>[2,3]</sup> It is commonly accepted that the effect of the bite angle on the reaction barrier of, for example, C–X bond activation [Eq. (1)], originates from an electronic factor.



According to this electronic model, the transition state (TS) is stabilized by donor–acceptor orbital interactions from metal d orbitals to the substrate  $\sigma_{\text{C-X}}^*$ , which become more stabilizing as the metal–ligand d hybrid orbital is pushed up at smaller bite angles.<sup>[3]</sup>

Here, we provide evidence that the mechanism through which the bite angle affects barrier heights (and also the twist angle in the TS, see Scheme 1)<sup>[4]</sup> is steric in nature, rather than electronic. This insight is of direct relevance for developing correct, rational design principles for catalysts. Our evidence is based on relativistic density functional

theory (DFT) analyses with the ADF program<sup>[5]</sup> at ZORA-BLYP/TZ2P (see reference [6] for benchmark studies) of a series of oxidative insertion (OxIn) reactions of model catalysts Pd, Pd(PH<sub>3</sub>)<sub>2</sub> and Pd[PH<sub>2</sub>(CH<sub>2</sub>)<sub>n</sub>PH<sub>2</sub>] (denoted as Pd-[PnP]) with  $n=1-6$  and model substrates H<sub>3</sub>C–X with X = H, CH<sub>3</sub>, and Cl.

To obtain a qualitative, physical understanding of how trends in catalytic activity (i.e., OxIn barrier height) are determined by the ligand and catalyst structure, we have carried out an analysis of the reaction profiles using the activation-strain model of chemical reactivity. In this model, the potential-energy surface  $\Delta E(\zeta)$  is decomposed, along the reaction coordinate  $\zeta$  (obtained from intrinsic reaction coordinate (IRC) calculations), into the strain associated with deforming the substrate,  $\Delta E_{\text{strain}}[\text{substr}](\zeta)$ , and the catalyst,  $\Delta E_{\text{strain}}[\text{cat}](\zeta)$ , plus the actual interaction  $\Delta E_{\text{int}}(\zeta)$  between these two deformed reactants [Eq. (2)]:<sup>[7–9]</sup>

$$\Delta E(\zeta) = \Delta E_{\text{strain}}[\text{substr}](\zeta) + \Delta E_{\text{strain}}[\text{cat}](\zeta) + \Delta E_{\text{int}}(\zeta) \quad (2)$$

Key results are collected in Table 1 and Figure 1; for details, see Tables S1 and S2 and Figure S1 in the Supporting Information.

A number of general trends can be observed in Tables 1 and S1. Both, the endothermicity and barrier height increase from Pd, along the series Pd[P1P] to Pd[P6P] and Pd(PH<sub>3</sub>)<sub>2</sub>. This is, in part, caused by a weakening of the catalyst–substrate interaction from bare to coordinated palladium, as suggested by the concomitant loss of stability of the reactant complexes and confirmed by our activation-strain analyses (vide infra). Furthermore, barrier heights increase from C–Cl to C–H to C–C activation, as discussed in detail already previously, for the insertion of uncoordinated Pd atoms.<sup>[7a]</sup>

The highly strained Pd[P1P], a four-membered ring, slightly expands (for insertion into C–H) or even fully dissociates (for insertion into C–C and C–Cl) one Pd–P bond in the reactant complexes and transition states. We have computed the reactions of Pd[P1P] as they occur (i.e., without any constraint), but also with the Pd–P dissociation suppressed through the constraint that both Pd–P bonds must be of equal length. The latter was done in order to allow for

[a] W. J. van Zeist, R. Visser, Prof. Dr. F. M. Bickelhaupt  
Department of Theoretical Chemistry and  
Amsterdam Center for Multiscale Modeling (ACMM)  
Scheikundig Laboratorium der Vrije Universiteit  
De Boelelaan 1083, 1081 HV Amsterdam (The Netherlands)  
Fax: (+31) 20-598-7629  
E-mail: fm.bickelhaupt@few.vu.nl

Supporting information for this article is available on the WWW  
under <http://dx.doi.org/10.1002/chem.200900367>.

Table 1. Geometry [in Å, °] and activation-strain analysis of transition states [in kcal mol<sup>-1</sup>] for Pd-induced C–X bond activation.<sup>[a]</sup>

H <sub>3</sub> C–H	bite <sup>[b]</sup>	twist	C–H	$\Delta E_{\text{int}}^{\ddagger}$	$\Delta E_{\text{strain}}^{\ddagger}$ [substr]	$\Delta E_{\text{strain}}^{\ddagger}$ [cat]	$\Delta E^{\ddagger}$	
Pd	–	(–)	–	1.62	–48.4	52.2	0.0	3.9
Pd[P1P] <sup>[c]</sup>	70	(78)	3	1.72	–49.3	62.1	3.9	16.8
Pd[P2P]	85	(98)	2	1.70	–48.4	61.0	6.0	18.6
Pd[P3P]	95	(115)	0	1.69	–46.7	59.9	9.0	22.2
Pd[P4P]	103	(131)	2	1.70	–46.3	60.9	11.0	25.7
Pd[P5P]	109	(146)	2	1.70	–45.6	60.6	14.2	29.2
Pd[P6P]	119	(156)	1	1.71	–44.5	61.2	15.3	32.1
Pd(PH <sub>3</sub> ) <sub>2</sub>	108	(180)	0	1.73	–47.8	63.3	16.7	32.2

H <sub>3</sub> C–CH <sub>3</sub>	bite <sup>[b]</sup>	twist	C–C	$\Delta E_{\text{int}}^{\ddagger}$	$\Delta E_{\text{strain}}^{\ddagger}$ [substr]	$\Delta E_{\text{strain}}^{\ddagger}$ [cat]	$\Delta E^{\ddagger}$	
Pd	–	(–)	–	1.95	–19.6	37.9	0.0	18.3
Pd[P1P] <sup>[c]</sup>	70	(78)	37	2.04	–16.1	47.4	3.4	34.7
Pd[P2P]	87	(98)	49	2.07	–16.7	50.7	4.3	38.4
Pd[P3P]	97	(115)	48	2.08	–15.1	51.4	6.8	43.1
Pd[P4P]	105	(131)	49	2.09	–14.6	52.6	8.3	46.3
Pd[P5P]	115	(146)	56	2.09	–13.7	52.8	10.5	49.5
Pd[P6P]	126	(156)	62	2.11	–13.3	53.6	11.2	51.5
Pd(PH <sub>3</sub> ) <sub>2</sub>	113	(180)	56	2.11	–15.8	53.7	13.4	51.3

H <sub>3</sub> C–Cl	bite <sup>[b]</sup>	twist	C–Cl	$\Delta E_{\text{int}}^{\ddagger}$	$\Delta E_{\text{strain}}^{\ddagger}$ [substr]	$\Delta E_{\text{strain}}^{\ddagger}$ [cat]	$\Delta E^{\ddagger}$	
Pd	–	(–)	–	2.05	–10.5	9.9	0.0	–0.6
Pd[P1P] <sup>[c]</sup>	72	(78)	22	2.17	–8.3	17.5	2.0	11.3
Pd[P2P]	89	(98)	43	2.21	–9.1	20.3	3.1	14.3
Pd[P3P]	101	(115)	48	2.22	–7.7	21.5	4.6	18.5
Pd[P4P]	111	(131)	52	2.23	–6.7	22.7	5.8	21.7
Pd[P5P]	128	(146)	72	2.25	–6.2	25.4	5.9	25.1
Pd[P6P]	137	(156)	88	2.24	–5.0	25.8	5.3	26.2
Pd(PH <sub>3</sub> ) <sub>2</sub>	123	(180)	68	2.25	–7.6	25.6	9.1	27.0

[a] Computed at ZORA-BLYP/TZ2P; see Equations (1) and (2). [PnP] = [PH<sub>2</sub>(CH<sub>2</sub>)<sub>n</sub>PH<sub>2</sub>]. [b] Bite angle in TS and, in parentheses, in isolated PdL<sub>2</sub>. [c] Transition states optimized under constraint of two equal Pd–P distances (see text).

a consistent analysis of how trends in activity of the cyclic model catalyst are affected by a monotonic decrease of its ring size (see Table 1). This constraint causes an artificial up-shift of the Pd[P1P]+CH<sub>3</sub>X barriers by 0.3, 7.7, and 8.8 kcal mol<sup>-1</sup> for C–H, C–C, and C–Cl (see Table S1). In the following, we discuss the results of the constrained Pd[P1P]+CH<sub>3</sub>X reactions in Table 1.

In all cases, there is a pronounced correlation between an increase of the bite angle in the model catalyst (values in parentheses in Table 1) and an increase in reaction barrier  $\Delta E^{\ddagger}$ . Thus, Pd(PH<sub>3</sub>)<sub>2</sub> has both the largest bite angle, 180°, and the highest barrier, whereas this barrier decreases monotonically as the number of methylene units in the model catalyst's bidentate ligand shrinks from *n* = 6 to 1 and forces the bite angle down to 78°. It is tempting, but incorrect, to attribute this correlation to the aforementioned electronic effect of a strengthening of the metal–substrate HOMO–LUMO interaction in the increasingly bent metal complex. Instead, our analyses reveal a steric origin of this and other correlations.

The main source of the barrier rise from Pd to Pd(PH<sub>3</sub>)<sub>2</sub> insertion is, in all cases, the increased activation strain  $\Delta E_{\text{strain}}^{\ddagger}$  (see Table 1). For example, from Pd to Pd(PH<sub>3</sub>)<sub>2</sub> +

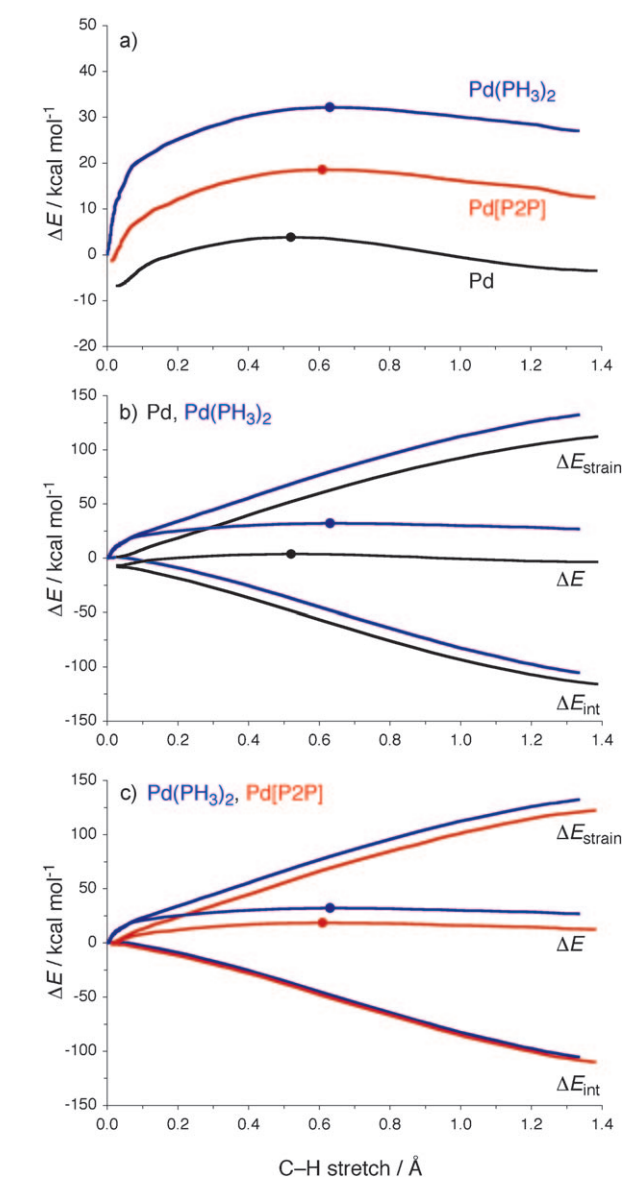


Figure 1. a) Reaction profiles and b,c) activation-strain diagrams of the oxidative insertion reactions of Pd (black), Pd(PH<sub>3</sub>)<sub>2</sub> (blue), and Pd[P2P] (red) with CH<sub>4</sub>. Dots indicate TS.

methane, the activation-strain terms  $\Delta E_{\text{strain}}^{\ddagger}$  [substr] and  $\Delta E_{\text{strain}}^{\ddagger}$  [cat] increase by some 10 and 17 kcal mol<sup>-1</sup>, respectively, whereas the catalyst–substrate interaction  $\Delta E_{\text{int}}^{\ddagger}$  is weakened by less than 1 kcal mol<sup>-1</sup>. Together, this yields the observed increase of the overall barrier by some 28 kcal mol<sup>-1</sup> (from 3.9 to 32.2 kcal mol<sup>-1</sup>). The strain of the methane substrate mainly stems from C–H bond expansion, with a slight contribution of the methyl-group tilting.<sup>[7a]</sup> On the other hand, the strain of the Pd(PH<sub>3</sub>)<sub>2</sub> model catalyst is generated nearly exclusively through the bending of the phosphine ligands, away from the substrate. This causes the P–Pd–P angle to decrease from 180° in the free Pd(PH<sub>3</sub>)<sub>2</sub> complex to 108° in the TS for insertion into the methane C–H bond.

Numerical experiments show that the energetically unfavorable geometrical deformation of the catalyst along the insertion process occurs in reaction to the even more destabilizing steric (Pauli) repulsion that occurs if the catalyst fragment would retain its linear geometry during the approach to the substrate (full details will be published elsewhere).<sup>[10]</sup> Similar effects occur for oxidative insertion into the ethane C–C and chloromethane C–Cl bonds. The Pd(PH<sub>3</sub>)<sub>2</sub> catalyst's activation strain  $\Delta E_{\text{strain}}^{\ddagger}[\text{cat}]$ , however, increases from 9.1 to 13.4 to 16.7 along C–Cl, C–C, and C–H bond activation, because, as discussed previously,<sup>[7b]</sup> the TS occurs still later on the reaction coordinate along this series. This translates into a relatively closer proximity in the TS between substrate and Pd(PH<sub>3</sub>)<sub>2</sub> complex, which therefore has to deform more strongly. This is also reflected by the bite angles in the TS which decrease, along C–Cl, C–C and C–H activation, from 123 to 113 to 108° (see Table 1).

Likewise, the twist angle decreases along the same series of substrates, for example, from 68 to 56 to 0° for the reaction of Pd(PH<sub>3</sub>)<sub>2</sub> + CH<sub>3</sub>Cl, CH<sub>3</sub>CH<sub>3</sub>, and CH<sub>4</sub>, respectively. This is so because transition states that occur later along the reaction coordinate more closely resemble the product complex [(Pd-d<sup>8</sup>)(L)<sub>2</sub>(CH<sub>3</sub>)(X)], which in all model reactions adopts a square-planar geometry. However, for a given substrate, the twist angle decreases systematically, together with the bite angle in Pd[PnP], along *n* = 6–1. For example, for the reactions of Pd[PnP] + CH<sub>3</sub>Cl the twist angle in the TS decreases from 88 to 22° along *n* = 6–1 (see Table 1). Numerical experiments reveal again a steric origin. Thus, as the steric demand decreases in the case of the smaller bite angles, the steric repulsion between ligands and substrate that causes the twisting is also reduced. Only in the case of C–H activation, is such a correlation between twist angle and bite angle absent, because here the twist angle is always close to 0°, as explained above. The present results highlight how the twist angle results from a balance of a steric effect, which induces twisting, and an electronic effect, which favors a planar arrangement (optimal  $\langle 4d_{\pi} | \sigma_{\text{C-X}}^* \rangle$  overlap, see Figure 2) and gains importance as the oxidative-insertion process progresses towards the product.

The above insights provide us with a clue for lowering the barrier  $\Delta E^{\ddagger}$  for oxidative insertion, namely, by deleting the catalyst's strain from the reaction profile. We can achieve

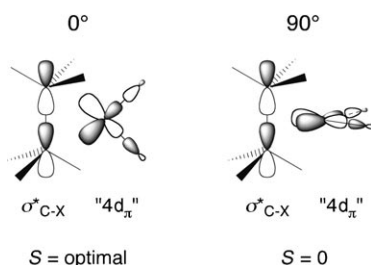


Figure 2. The  $\langle 4d_{\pi} | \sigma_{\text{C-X}}^* \rangle$  overlap is optimal for a twist angle of 0° (left) and minimal for a twist angle of 90° (right). This overlap and the corresponding orbital interaction gain importance as the reaction advances.

this by constructing a catalyst complex that is already bent from the beginning and into which the bending strain is thus already built-in. This is exactly what happens if we go from individual phosphine ligands in Pd(PH<sub>3</sub>)<sub>2</sub> to the bidentate ligands in Pd[PnP]. Thus, along the series for *n* = 6–1, the bite angle decreases and forces the phosphine groups away from the substrate. Consequently, there is less steric contact between ligands and substrate. This is nicely reflected by the reduced need for additional bending in the TS and, accordingly a drop in catalyst activation strain  $\Delta E_{\text{strain}}^{\ddagger}[\text{cat}]$ , for example, from 16.7 and 15.3 kcal mol<sup>-1</sup> for Pd(PH<sub>3</sub>)<sub>2</sub>- and Pd-[P6P]-induced C–H activation down to only 3.9 kcal mol<sup>-1</sup> for Pd[P1P]-induced C–H activation. Note that this drop of approximately 13 kcal mol<sup>-1</sup> in  $\Delta E_{\text{strain}}^{\ddagger}[\text{cat}]$  accounts for most of the concomitant reduction in the barrier  $\Delta E^{\ddagger}$  by some 15 kcal mol<sup>-1</sup>, from 32.2 down to 16.8 kcal mol<sup>-1</sup>.

Interestingly, we do in fact see a slight rise in orbital energy of the 4d<sub>π</sub>-derived metal–ligand hybrid orbital that donates charge into the C–X antibonding  $\sigma_{\text{C-X}}^*$  orbital of the substrate, in line with the aforementioned electronic bite-angle model.<sup>[3]</sup> However, the rise in orbital energy is not large, only 0.5 eV as we subject the Pd(PH<sub>3</sub>)<sub>2</sub> fragment to a rigid bending of the bite angle over a substantial range of 40°, from 120 to 80°. Accordingly, the changes in catalyst–substrate TS interaction are negligible along the series of model catalysts. For example, from Pd(PH<sub>3</sub>)<sub>2</sub> to Pd-[P1P] + CH<sub>4</sub>, the TS interaction  $\Delta E_{\text{int}}^{\ddagger}$  is strengthened by only 1.5 kcal mol<sup>-1</sup>, from –47.8 to –49.3 kcal mol<sup>-1</sup> (see Table 1).

The steric nature of the bite angle that emerges from the above analyses of transition states is confirmed if we, more rigorously, extend the activation-strain analyses along the entire reaction coordinate. Figure 1 shows three representative reactions of methane C–H bond activation: a) by bare Pd, b) by Pd(PH<sub>3</sub>)<sub>2</sub>, and c) by Pd[P2P]; similar activation-strain diagrams are found for ethane C–C and chloromethane C–Cl bond activation (see Figure S1).

The reaction profiles in Figure 1a show again the dramatic increase by almost 30 kcal mol<sup>-1</sup> from uncoordinated Pd (black curve) to Pd(PH<sub>3</sub>)<sub>2</sub> (blue curve) and the substantial drop in energy from Pd(PH<sub>3</sub>)<sub>2</sub> to the geometrically confined Pd[P2P] complex with its small bite angle (red curve). Comparison of the activation-strain diagrams of Pd and Pd(PH<sub>3</sub>)<sub>2</sub> + CH<sub>4</sub> in Figure 1b reveals that the main reason for the higher reaction barrier for Pd(PH<sub>3</sub>)<sub>2</sub> is a substantial destabilization of the strain curve  $\Delta E_{\text{strain}}^{\ddagger}$ . A weakening in the interaction curve  $\Delta E_{\text{int}}^{\ddagger}$  also contributes, but is almost two times smaller. Finally, comparison of the activation-strain diagrams of Pd(PH<sub>3</sub>)<sub>2</sub> and Pd[P2P] + CH<sub>4</sub> in Figure 1c reveals that the accompanying drop in reaction barrier is indeed nearly exclusively caused by a corresponding reduction in the strain curve. Note that the interaction curves for Pd(PH<sub>3</sub>)<sub>2</sub> and Pd[P2P] practically coincide!

This confirms the steric nature of bite-angle effects, as well as the idea of taking away destabilizing strain from the reaction profile by building it, right from the beginning, into the catalytically active transition metal complex. In view of

the fact that bite-angle tuning is a central paradigm in modern catalyst design, the insights obtained in this work may serve a more rational development and optimization of catalysts, with the correct (steric) working mechanism of this design parameter in mind.

### Acknowledgements

We thank the National Research School Combination-Catalysis (NRSC-C) and the Netherlands Organization for Scientific Research (NWO-CW) for financial support.

**Keywords:** activation-strain model • bite angle • density functional calculations • homogeneous catalysis • oxidative addition

- [1] P. W. N. M. van Leeuwen, P. C. J. Kamer, J. N. H. Reek, P. Dierkes, *Chem. Rev.* **2000**, *100*, 2741.
- [2] a) S. Otsuka, *J. Organomet. Chem.* **1980**, *200*, 191; b) J. J. Low, W. A. Goddard, *J. Am. Chem. Soc.* **1984**, *106*, 6928; c) P. Hofmann, H. Heiss, G. Müller, *Z. Naturforsch. B* **1987**, *42*, 395; d) P. Dierkes, P. W. N. M. van Leeuwen, *J. Chem. Soc. Dalton Trans.* **1999**, 1519; e) Z. Freixa, P. W. N. M. van Leeuwen, *Dalton Trans.* **2003**, 1890; f) R. Fazaeli, A. Ariafard, S. Jamshidi, E. S. Tabatabaie, K. A. Pishro, *J. Organomet. Chem.* **2007**, *692*, 3984; g) V. P. Ananikov, D. G. Musaev, K. Morokuma, *Eur. J. Inorg. Chem.* **2007**, 5390.
- [3] a) S. Sakaki, B. Biswas, M. Sugimoto, *J. Chem. Soc. Dalton Trans.* **1997**, 803; M. D. Su, S. Y. Chu, *Inorg. Chem.* **1998**, *37*, 3400; b) S. Kozuch, C. Amatore, A. Jutand, S. Shaik, *Organometallics* **2005**, *24*, 2319.
- [4] a) S. Sakaki, N. Mizoe, Y. Musashi, B. Biswas, M. Sugimoto, *J. Phys. Chem. A* **1998**, *102*, 8027; b) T. Matsubara, K. Hirao, *Organometallics* **2002**, *21*, 4482.
- [5] a) E. J. Baerends, J. Autschbach, J. A. Berger, A. Bérces, F. M. Bickelhaupt, C. Bo, P. L. de Boeij, P. M. Boerrigter, L. Cavallo, D. P. Chong, L. Deng, R. M. Dickson, D. E. Ellis, M. van Faassen, L. Fan, T. H. Fischer, C. Fonseca Guerra, S. J. A. van Gisbergen, A. W. Götz, J. A. Groeneveld, O. V. Gritsenko, M. Grüning, F. E. Harris, P. van den Hoek, C. R. Jacob, H. Jacobsen, L. Jensen, E. S. Kadantsev, G. van Kessel, R. Klooster, F. Kootstra, M. V. Krykunov, E. van Lenthe, J. N. Louwen, D. A. McCormack, A. Michalak, J. Neugebauer, V. P. Nicu, V. P. Osinga, S. Patchkovskii, P. H. T. Philipsen, D. Post, C. C. Pye, W. Ravenek, J. I. Rodríguez, P. Romaniello, P. Ros, P. R. T. Schipper, G. Schreckenbach, J. G. Snijders, M. Solà, M. Swart, D. Swerhone, G. te Velde, P. Vernooijs, L. Versluis, L. Visscher, O. Visser, F. Wang, T. A. Wesolowski, E. M. van Wezenbeek, G. Wiesenekker, S. K. Wolff, T. K. Woo, A. L. Yakovlev, T. Ziegler, ADF2008.01, SCM, Amsterdam, **2007**; b) G. te Velde, F. M. Bickelhaupt, E. J. Baerends, C. Fonseca Guerra, S. J. A. van Gisbergen, J. G. Snijders, T. Ziegler, *J. Comput. Chem.* **2001**, *22*, 931.
- [6] a) G. T. de Jong, M. Solà, L. Visscher, F. M. Bickelhaupt, *J. Chem. Phys.* **2004**, *121*, 9982; b) G. T. de Jong, D. P. Geerke, A. Diefenbach, F. M. Bickelhaupt, *Chem. Phys.* **2005**, *313*, 261; c) G. T. de Jong, D. P. Geerke, A. Diefenbach, M. Solà, F. M. Bickelhaupt, *J. Comput. Chem.* **2005**, *26*, 1006; d) G. T. de Jong, F. M. Bickelhaupt, *J. Chem. Theory Comput.* **2006**, *2*, 322.
- [7] a) G. T. de Jong, F. M. Bickelhaupt, *ChemPhysChem* **2007**, *8*, 1170; b) W. J. van Zeist, C. Fonseca Guerra, F. M. Bickelhaupt, *J. Comput. Chem.* **2008**, *29*, 312; c) W. J. van Zeist, A. H. Koers, L. P. Wolters, F. M. Bickelhaupt, *J. Chem. Theory Comput.* **2008**, *4*, 920.
- [8] For early work on the activation-strain model, see: a) F. M. Bickelhaupt, *J. Comput. Chem.* **1999**, *20*, 114; b) F. M. Bickelhaupt, N. M. M. Nibbering, E. J. Baerends, T. Ziegler, *J. Am. Chem. Soc.* **1993**, *115*, 9160; other studies in which the reactant strain or distortion energy have been separated from the interaction energy for understanding chemical reactions are, for example: c) D. J. Mitchell, H. B. Schlegel, S. S. Shaik, S. Wolfe, *Can. J. Chem.* **1985**, *63*, 1642; d) C. Y. Legault, Y. Garcia, C. A. Merlic, K. N. Houk, *J. Am. Chem. Soc.* **2007**, *129*, 12664.
- [9] a) T. Ziegler, A. Rauk, *Theor. Chim. Acta* **1977**, *46*, 1; b) F. M. Bickelhaupt, E. J. Baerends in *Reviews in Computational Chemistry, Vol. 15* (Eds.: K. B. Lipkowitz, D. B. Boyd), Wiley-VCH, Weinheim, **2000**, pp. 1–86.
- [10] In our quantitative (Kohn–Sham) molecular orbital (MO) approach, the steric repulsion is defined as the Pauli repulsion between same-spin orbitals, for example, the two-orbital four-electron repulsion. In contrast, electronic effects in our MO analysis are defined as the stabilizing orbital interactions that stem from relaxation effects, such as donor–acceptor interactions, including the HOMO–LUMO interactions. In the present case, they cover donation and back-donation between the palladium catalyst and the substrate. For details, see reference [9b].

Received: February 10, 2009  
Published online: May 21, 2009